Computational Mathematics and Mathematical Physics, Vol. 41, No. 4, 2001, pp. 609–621.
Translated from Zhurnal Vychislitel'noi Matematiki i Matematicheskoi Fiziki, Vol. 41, No. 4, 2001, pp. 648–661.

Dynamic Adaptation Method for a Laminar Combustion Problem

M. M. Demin, V. I. Mazhukin, and A. V. Shapranov

Institute of Mathematical Modeling, Russian Academy of Sciences, Miusskaya pl. 4a, Moscow, 125047 Russia
e-mail: immras@ors.ru

Received March 29, 2000

Abstract—A method for constructing grids dynamically adapting to solutions is applied to problems with unstable (relaxation or oscillatory) solution behavior. Numerical simulation is used to analyze steady and pulsating modes of laminar combustion in wide ranges of Lewis numbers and activation energies. The efficiency of the method is estimated in terms of its time complexity and the number of nodes employed. The numerical simulation shows that dynamic adaptation reduces the number of grid nodes by 1–2.5 orders of magnitude and the time complexity by a factor of 2–50.

INTRODUCTION

The practice of numerical simulation [1–5] demonstrates that the application of grids adapting to solutions substantially increases the efficiency of computational algorithms, resulting in a substantial increase in solution accuracy and a simultaneous reduction of the number of grid nodes. Such grids are particularly efficient when employed in solving time-dependent problems with fast-moving narrow zones of steep gradients, such as the problem of subsonic laminar flame propagation. The high rate of chemical transformation of a reactant and the slow propagation of thermal perturbations in the unreacted mixture result in the formation of a narrow combustion zone characterized by steep gradients of temperature and concentration.

The main problem in the theoretical studies of combustion processes is the determination of the normal velocity and regime of flame propagation. One of the most important factors affecting the propagation regime of the flame front in the problem of laminar (layer-by-layer) combustion (frontal combustion) is the relation between the transport coefficients, the species diffusivity D and thermal diffusivity α. Depending on their ratio (the ratio of D to α is known as the Lewis number $\mathrm{Le} = D/\alpha$), the combustion proceeds in a steady ($\mathrm{Le} = 1$) or pulsating ($\mathrm{Le} \neq 1$) regime (see [6]). Steady regimes are characterized by constant front propagation velocities and stable thermodiffusional flame structures. The onset of a thermodiffusional instability involves a violation of the similarity between the temperature and concentration distributions, and the front velocity can exhibit a complicated pulsating pattern. The more the Lewis number deviates from unity, the stronger are the manifestations of the instability. The equality $\mathrm{Le} = 0$ formally corresponds to the combustion of a condensed substance. Numerous theoretical studies [7–11] have been devoted to the determination of conditions for the thermal stability of the combustion of condensed substances and for the thermodiffusional stability of gas combustion. However, numerical simulation of unstable and self-sustained oscillatory regimes remains a difficult computational problem [3]. In particular, grids with huge numbers of nodes are required [11].

From a computational perspective, combustion problems are specific in that they involve processes with widely different characteristic times: a short chemical reaction time and the long time associated with the diffusive mechanism of thermal relaxation. Accordingly, the high rate of chemical transformations in the substance and the slow propagation of thermal disturbances and diffusion in the reactive mixture result in the formation of a narrow combustion zone with steep gradients of temperature T and density ρ. The combustion front appears at one of the boundaries and quickly moves toward the opposite one. In a numerical solution, a certain number of grid nodes must lie in the reaction zone. These two features preclude using grids with fixed nodes to discretize space variables with a large step. When the ratio of the domain size to the typical width of the combustion zone is large, the efficiency of computational algorithms with fixed grids rapidly deteriorates because of the large number of nodes required. For example, the conventional grid contains 3000–5000 fixed nodes in a typical problem of unstable combustion [11]. In this situation, grids that dynamically adapt to a solution are much more efficient, since a necessary number of nodes is concentrated in the zones of rapid variation.

The dynamically adaptive method proposed in [12–14] for solving time-dependent problems has proved to be highly efficient as applied to moving-boundary problems with steep solution gradients. It can be used to solve problems by automatically capturing strong discontinuities, such as phase boundaries in multiple-front Stefan problems [15, 16] and shock waves in gas dynamics [17]. In problems of the Burgers type, the application of dynamic adaptation [18] allows one to substantially improve the quality of difference schemes by nearly eliminating their dispersive properties and considerably reducing dissipation. Eventually, this made it possible to reduce the number of nodes by two to three orders of magnitude as compared to grids with fixed nodes. However, the dynamic adaptation method in which the transformation function is determined by applying the quasistationarity principle has never been applied to problems with oscillatory solutions.

In this study, we extend the dynamic adaptation to mathematical models of various stable, unstable, and oscillatory regimes of laminar combustion and determine the efficiency of the method in terms of time complexity and number of nodes employed.

1. MATHEMATICAL FORMULATION OF THE PROBLEM

The physical mechanism of flame propagation in a quiescent gaseous mixture is dominated by heat transfer from the high-temperature burned gas to the unreacted gas. Consider a quiescent gas that is homogeneous in terms of temperature and concentration. The propagation of an exothermic reaction front in this medium is considered in the simplest case of a single-stage combustion, with the heat release function of a first-order chemical reaction, Φ, expressed in the form

$$\Phi(\tilde{T}, \tilde{\rho}) = h\tilde{\rho}ke^{-E/R\tilde{T}}, \tag{1}$$

where h is the heat of reaction per unit mass, k is the rate constant, E is the activation energy, and R is the gas constant.

Thus, the heat release rate of an exothermic reaction depends linearly on the medium density $\tilde{\rho}$ and exponentially (according to the Arrhenius law) on the temperature $\tilde{T}$, which is consistent with the modern theory of chemical reaction kinetics in homogeneous media. Assuming that the combustion process is isobaric and heat is transferred through diffusion, one can describe laminar flame propagation by a system of two parabolic differential equations, the heat and diffusion equations with constant thermal and species diffusivities, α and D, respectively. The dimensional formulation of the problem in the physical space $\Omega_{\tilde{x}\tilde{t}}$ has the form

$$C_p\rho_0\frac{\partial\tilde{T}}{\partial\tilde{t}} = \lambda\frac{\partial^2\tilde{T}}{\partial\tilde{x}^2} + h\tilde{\rho}k\exp\left(-\frac{E}{R\tilde{T}}\right), \tag{2}$$

$$\frac{\partial\tilde{\rho}}{\partial t} = D\frac{\partial^2\tilde{\rho}}{\partial\tilde{x}^2} - \tilde{\rho}k\exp\left(-\frac{E}{R\tilde{T}}\right), \tag{3}$$

$$0 = \tilde{x}_0 \le \tilde{x} \le \tilde{x}_1 = L, \quad \tilde{t} \ge 0,$$

where $\tilde{t}$ and $\tilde{x}$ are time and coordinate, respectively; D, λ, C_p, and ρ_0 are species diffusivity, heat conductivity, specific heat, and initial density of the substance, respectively; and L is the length of the domain under consideration.

Initial and boundary conditions. In choosing the value of L, we took into account the fact that the typical size of the combustion chamber in an internal combustion engine is ≈5 cm. As a rule, the value of L used in calculations did not exceed 10 cm.

Normally, a chemical reaction in a substance is initiated at a boundary by means of an external energy source, and a reaction front propagates toward the opposite boundary. Suppose that the source is a hot wall located at $\tilde{x} = 0$. Its temperature varies linearly from an initial temperature $\tilde{T}_0$ to a so-called adiabatic flame temperature $\tilde{T}_a = \tilde{T}_0 + h/C_p$, $\tilde{T}_0 \le \tilde{T} \le \tilde{T}_a$. The mass flux across the left boundary was assumed to be zero. These assumptions correspond to the following relations:

$$\tilde{T}(0, \tilde{t}) = \tilde{T}_0 + c\tilde{t}, \quad -D\frac{\partial\tilde{\rho}(0, \tilde{t})}{\partial\tilde{x}} = 0, \quad \tilde{x} = \tilde{x}_0 = 0. \tag{4}$$

The opposite wall at $\tilde{x} = \tilde{x}_L$ is assumed to be thermally and diffusionally insulated:

$$-\lambda\frac{\partial\tilde{T}(\tilde{x}_L, \tilde{t})}{\partial\tilde{x}} = 0, \quad -D\frac{\partial\tilde{\rho}(\tilde{x}_L, \tilde{t})}{\partial\tilde{x}} = 0, \quad \tilde{x} = \tilde{x}_L = L. \tag{5}$$

The initial temperatures $\tilde{T}(x, 0)$ were chosen by using the fact that the heat release rate (1) practically vanishes at $\tilde{T}_0$. The initial density $\tilde{\rho}(x, 0)$ was set equal to the unperturbed-gas density ρ_0:

$$\tilde{T}(x, 0) = \tilde{T}_0, \quad \tilde{\rho}(x, 0) = \rho_0, \quad \tilde{t} = 0. \tag{6}$$

For numerical convenience, problem (2)–(6) was reduced to a dimensionless form by introducing the following dimensionless variables:

$$\rho = \frac{\tilde{\rho}}{\rho_0}, \quad x = \frac{\tilde{x}}{\tilde{L}}, \quad t = \frac{\tilde{t}\alpha}{L^2}, \quad T = \frac{\tilde{T}C_p}{h}, \quad \theta = \frac{EC_p}{Rh}, \quad A = \frac{kL^2}{a}, \quad \alpha = \frac{\lambda}{C_p\rho_0}, \quad \mathrm{Le} = \frac{D}{\alpha},$$

where θ is the dimensionless activation energy, and A is the preexponential factor.

In dimensionless form, equations (2) and (3) are written as

$$\frac{\partial T}{\partial t} = \frac{\partial^2 T}{\partial x^2} + \rho A\exp\left(-\frac{\theta}{T}\right), \tag{7}$$

$$\frac{\partial \rho}{\partial t} = \mathrm{Le}\frac{\partial^2 \rho}{\partial x^2} - \rho A\exp\left(-\frac{\theta}{T}\right), \tag{8}$$

where $0 = x_0 \le x \le x_1 = 1$, $t \ge 0$, $(x, t) \in \Omega_{xt}$. The initial and boundary conditions in the space Ω_{xt} are

$$T(x, 0) = T_0, \quad \rho(x, 0) = \rho_0, \quad t = 0,$$

$$T(x_0, t) = \begin{cases} T_0 + ct, & t \le 1/c, \\ T_a, & t > 1/c, \end{cases} \quad -D\frac{\partial\rho}{\partial x} = 0, \quad x = x_0 = 0, \tag{9}$$

$$-\lambda\frac{\partial T}{\partial x} = 0, \quad -D\frac{\partial\rho}{\partial x} = 0, \quad x = 1,$$

where c is a constant.

In these equations, ρ varies from unity to zero. In the absence of external heat sources, the value of the dimensionless temperature T lies in the interval $T_0 \le T \le T_a$, where $T_a = 1 + T_0$. The parameter values adopted in this paper are similar to those used in [19] for the combustion of hydrocarbon fuel in air, which is characterized by a sixfold increase in temperature. Therefore, the value $T_0 = 0.2$ is taken as the initial condition in most cases, which implies $T_a/T_0 = 6$. Typical values of the dimensionless activation energy for the reactions of hydrocarbons in air are $\theta = 3$–6.

2. ARBITRARY TIME-DEPENDENT COORDINATE SYSTEM AND CONSTRUCTION OF DYNAMICALLY ADAPTIVE GRIDS

Let us use the dynamic adaptation method [12, 13], in which the mesh is constructed by changing to an arbitrary time-dependent coordinate system with variables (q, τ) belonging to some computational space $\Omega_{q\tau}$. The transformation of coordinates is performed by using the desired solution. The partial differential equation of the inverse transformation is constructed so that the velocities of the nodes depend on the dynamics of the solutions to the equations describing the physical processes.

The change from a physical space Ω_{xt} to a computational one $\Omega_{q\tau}$ is defined by a coordinate transformation of the general form $x = \xi(q, \tau)$, $t = \tau$, which has an inverse transformation $q = \varphi(x, t)$, $\tau = t$. The Jacobian

of this transformation is $\psi = \partial x/\partial q$. The partial derivatives of the dependent variables are expressed in a standard form:

$$\frac{\partial}{\partial t} = \frac{\partial}{\partial \tau} + \frac{\partial q}{\partial t}\frac{\partial}{\partial q} = \frac{\partial}{\partial \tau} - \frac{\partial x}{\partial \tau}\frac{1}{\psi}\frac{\partial}{\partial q} = \frac{\partial}{\partial \tau} + \frac{Q}{\psi}\frac{\partial}{\partial q},$$

$$\frac{\partial}{\partial x} = \frac{\partial q}{\partial x}\frac{\partial}{\partial q} = \frac{1}{\psi}\frac{\partial}{\partial q}, \quad \frac{\partial^2}{\partial x^2} = \frac{\partial q}{\partial x}\frac{\partial}{\partial q}\frac{\partial q}{\partial x}\frac{\partial}{\partial q} = \frac{1}{\psi}\frac{\partial}{\partial q}\frac{1}{\psi}\frac{\partial}{\partial q},$$

where $\partial x/\partial \tau = -Q$ is the velocity of the motion of the time-dependent coordinate system. In the new variables (q, τ), problem (7)–(9) can is written as

$$\frac{\partial T}{\partial \tau} = -\frac{1}{\psi}\frac{\partial W}{\partial q} - \frac{Q}{\psi}\frac{\partial T}{\partial q} + \rho A \exp\left(-\frac{\theta}{T}\right), \quad W = -\frac{1}{\psi}\frac{\partial T}{\partial q}, \tag{10}$$

$$\frac{\partial \rho}{\partial \tau} = -\mathrm{Le}\frac{1}{\psi}\frac{\partial J}{\partial q} - \frac{Q}{\psi}\frac{\partial \rho}{\partial q} - \rho A \exp\left(-\frac{\theta}{T}\right), \quad J = -\frac{1}{\psi}\frac{\partial \rho}{\partial q}, \tag{11}$$

$$\partial \psi/\partial \tau = -\partial Q/\partial q, \quad \partial x/\partial q = \psi, \quad 0 = q_0 \le q \le q_L = L, \quad \tau \ge 0. \tag{12}$$

By changing to an arbitrary time-dependent system, we obtain an extended system of differential equations in which Eq. (12) can be used for constructing an adaptive grid after the form of Q is determined.

In the space $\Omega_{q\tau}$, initial and boundary conditions (9) have the form

$$T(q, 0) = T_0, \quad \rho(q, 0) = \rho_0, \quad \tau = 0,$$

$$T(q_0, \tau) = \begin{cases} T_0 + c\tau, & \tau \le 1/c, \\ T_a, & \tau > 1/c, \end{cases} \quad -\frac{1}{\psi}\frac{\partial \rho}{\partial q} = 0, \quad q = q_0 = 0, \tag{13}$$

$$-\frac{1}{\psi}\frac{\partial T}{\partial q} = 0, \quad -\frac{1}{\psi}\frac{\partial \rho}{\partial q} = 0, \quad q = q_L = 1.$$

Since the boundaries of the physical domain are stationary, the boundary conditions for the supplementary equation (12) correspond to a vanishing function Q:

$$Q(q_0, \tau) = Q(q_L, \tau) = 0. \tag{14}$$

Here, the function Q remains arbitrary. Its definition determines a specific form of the coordinate transformation used to control of the motion of grid nodes.

3. TRANSFORMATION FUNCTION Q

In the general case, the coordinate transformation should be such that the solution gradients in the computational space are much lower than those in the physical space. A proper choice of the transformation function Q ensures that the motion of the nodes is consistent with the solution. This is one of the most important principles in the dynamic adaptation method. If the motion of the nodes is not sufficiently fast, then their condensation will not keep pace with the displacement of solution singularities, and the adaptation efficiency will be lower. When the nodes move too fast, the solution will oscillate, or coupled oscillations of the grid and solution will develop, or the calculations will become globally unstable.

Generally, to compensate for the incomplete consistency of the required solution with the mechanism of grid adaptation, coefficients are introduced into the transformation function, which are adjusted so as to reduce the degree of inconsistency. At the same time, the use of adjusted coefficients in an adaptation method is indicative of its imperfection.

To determine the necessary transformation function, we use the quasistationarity principle formulated in [17]. It can be applied to determine the transformation functions that are free of adjustable parameters [17, 18]. The quasistationarity principle is based on the assumption that there exists a time-dependent coordinate system in which all processes are steady; i.e., the time derivatives of a solution vanish or are suffi-

ciently small. Extending the quasistationarity principle to system (10)–(12), we suppose that there exists a coordinate system in which $\partial T/\partial\tau = \partial\rho/\partial\tau = 0$. Then, (10)–(12) imply

$$\frac{Q}{\psi}\frac{\partial T}{\partial q} + \frac{1}{\psi}\frac{\partial W}{\partial q} - \rho A\exp\left(-\frac{\theta}{T}\right) = 0, \tag{15}$$

$$\frac{Q}{\psi}\frac{\partial \rho}{\partial q} + \mathrm{Le}\frac{1}{\psi}\frac{\partial J}{\partial q} + \rho A\exp\left(-\frac{\theta}{T}\right) = 0. \tag{16}$$

Solving (15) and (16) for Q, we obtain the desired transformation function

$$Q = \frac{1}{\psi}\left(\mathrm{Le}\frac{\partial}{\partial q}\left|\frac{\partial\rho}{\partial q}\right| + \frac{\partial}{\partial q}\left|\frac{\partial T}{\partial q}\right|\right)\left(\left|\frac{\partial}{\partial q}(\rho + T)\right| + \mathrm{reg}\right)^{-1} + \left(\frac{\partial}{\partial q}\frac{1}{\psi}\right)\left(\mathrm{Le}\left|\frac{\partial\rho}{\partial q}\right| + \left|\frac{\partial T}{\partial q}\right|\right)\left(\left|\frac{\partial}{\partial q}(\rho + T)\right| + \mathrm{reg}\right)^{-1}. \tag{17}$$

The first summand in this formula is responsible for grid condensation, and the second one sets a finite limit for the distance between two adjacent nodes. Since the solution is not monotone, we take the absolute values of the first derivatives of density and temperature. The constant $\mathrm{reg} \ll 1$ prevents the denominator from vanishing at the points where the spatial derivatives vanish.

To solve system (10)–(12) numerically, it should be represented in a strictly conservative form:

$$\frac{\partial(\psi T)}{\partial\tau} = -\frac{\partial W}{\partial q} - \frac{\partial(QT)}{\partial q} + \psi\rho A\exp\left(-\frac{\theta}{T}\right), \tag{18}$$

$$\frac{\partial(\psi\rho)}{\partial\tau} = -\mathrm{Le}\frac{\partial J}{\partial q} - \frac{\partial(Q\rho)}{\partial q} - \psi\rho A\exp\left(-\frac{\theta}{T}\right), \tag{19}$$

$$\partial\psi/\partial\tau = -\partial Q/\partial q, \quad \partial x/\partial q = \psi. \tag{20}$$

4. MODIFICATION OF BOUNDARY CONDITIONS

To improve the efficiency of the dynamic adaptation, we modify boundary conditions (14) so that problem (18)–(20) is reformulated as a free-boundary problem [3, 20]. Since the combustion process is initiated at the left boundary $q = q_0$, and the combustion wave propagates across a cold background toward the right boundary $q = q_L$, it is reasonable to exclude the unperturbed region from the analysis by formulating boundary conditions on the right boundary so that the starting problem is posed as a free-boundary problem. To do this, we set a new boundary at an arbitrary point $q_* \in (q_0, q_L)$ such that $q_* > q_0$ and $q_* \ll q_L$ and formulate the corresponding boundary conditions as in [3, 20]:

$$T(q_*, \tau) = T_0, \quad \rho(q_*, \tau) = \rho_0, \quad Q(q_*, \tau) = u = \lim_{q\to q_*} -\frac{a}{T}\frac{1}{\psi}\frac{\partial T}{\partial q}. \tag{21}$$

Until the perturbation reaches the point $q = q_*$, the boundary remains at rest. Its motion begins when the heat wave arrives and ceases when the wave reaches the point $q = q_L$. In the final form, the boundary and initial conditions for equations (18)–(20) are written as

$$T(q, 0) = T_0, \quad \rho(q, 0) = \rho_0, \quad \psi(q, 0) = 1, \quad \tau = 0,$$

$$T(q_0, \tau) = \begin{cases} T_0 + c\tau, & \tau \le 1/c, \\ T_a, & \tau > 1/c, \end{cases} \quad -\frac{1}{\psi}\frac{\partial\rho}{\partial q} = 0, \quad Q(q_0, \tau) = 0, \quad q = q_0 = 0, \tag{22}$$

$$T(q_*, \tau) = T_0, \quad \rho(q_*, \tau) = \rho_0, \quad Q(q_*, \tau) = u = \lim_{q\to q_*} -\frac{a}{T}\frac{1}{\psi}\frac{\partial T}{\partial q}, \quad q = q_* = L_*.$$

5. SIMULATION OF STABLE AND UNSTABLE COMBUSTION REGIMES

Studies of various combustion regimes are generally focused on the calculation of the normal propagation velocity u and the thermodiffusional structure of the flame front. The numerical analysis of flame front propagation and structure concentration and temperature fields was performed by using both mathematical models, (7)–(9) and (18)–(22), which are formulated in the stationary (x, t) and time-dependent (q, τ) coor-

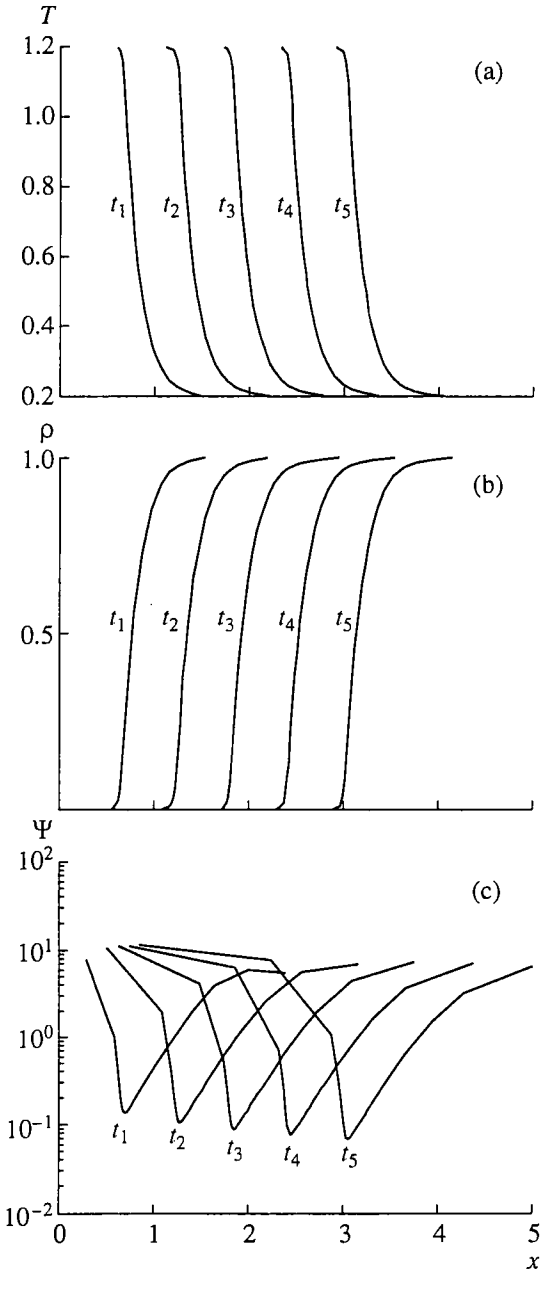

Fig. 1.

dinate systems, respectively. The combustion model (7)–(9), formulated in the variables (x, t), was mainly used to compare the results and determine the efficiency of the dynamic adaptation method. Equations (18)–(22) were solved to determine the spatiotemporal distributions of temperature $T(x, t)$, density $\rho(x, t)$, the preheat-zone width $\delta_T(t)$ and the reaction-zone width $\delta_\rho(t)$, as well as the flame propagation velocity $u(t)$.

Differential models (7)–(9) and (18)–(22) were approximated by difference schemes constructed by means of the integro-interpolation method [21]. In both models, symmetric conservative difference schemes with $O(\Delta t^2 + \Delta h_x^2)$ and $O(\Delta\tau^2 + \Delta h_q^2)$ errors were used, where Δt, Δh_x, $\Delta\tau$, and Δh_q are the integration steps in t, x, τ, and q, respectively.

At the beginning of each calculation, a linear law of temperature rise on the left boundary was assumed. As the temperature on this boundary grows, the chemical reaction rate steeply increases. The heat released in the course of the reaction induces a temperature gradient, which gives rise to a rapidly increasing inward heat flux. As a result, the combustion zone begins to move quickly toward the right boundary. The regime of further propagation of the flame front depends on the values of several parameters. In the case of a gaseous medium, these parameters include the Lewis number Le. Combustion in condensed media formally corresponds to Le = 0, the reaction zone structure depends only on the thermal diffusivity α.

Experimental [6, 21] and theoretical [7, 10] studies of combustion in gaseous media have shown that, depending on the relation between the coefficients Le and α, there exist two qualitatively different regimes characterized by stable or unstable propagation of the reaction front. In one of them, with $\mathrm{Le} = D/\alpha \approx 1$, the one-dimensional combustion process is stable. This regime is characterized by spatial profiles $T(x, t)$ and $\rho(x, t)$ that propagate with a constant speed, while the flame front is plane and has a stable thermodiffusional structure. In the other regime, when $\alpha = (T_a - T_0)d(\ln u)/dT_0 > \alpha_c$, where α_c is a critical value, T_a is the adiabatic temperature, and Le < 1, the so-called one-dimensional thermodiffusional instability develops [6, 10], and combustion proceeds in an oscillatory mode. It was found that, in the case of a two-dimensional flame, the conditions of thermodiffusional instability [7] are opposite: the flame is stable for Le < 1 and unstable for Le > 1.

Steady combustion regime. As we mentioned above, steady combustion regimes correspond to $\mathrm{Le} \approx 1$. After the influence of the left boundary condition (heating wall) becomes small; i.e., starting from the moment when equilibrium between the conductive heat flux from the reaction zone and the heat release due to the chemical reaction is reached, the reaction zone starts moving rightwards with a constant speed. Combustion proceeds in a steady regime, with typical profiles of temperature $T(x)$, density $\rho(x)$, and the function $\psi(x)$ shown in Fig. 1 for Le = 1, $\theta = 18$, and $A = 10^{10}$. Figure 2 shows the combustion rate $u(t)$, preheat-zone width $\delta_T(t)$ and reaction-zone width $\delta_\rho(t)$ plotted for the same values of parameters. The trajectories of grid nodes $x_i(t)$ are illustrated by Fig. 3. Combustion at Le = 1, $\theta = 18$, $A = 10^{10}$ is special in that the maximum temperature equals the adiabatic combustion temperature: $T_m = T_a (T_a = T_0 + \Phi/C_p)$. The thermal front width

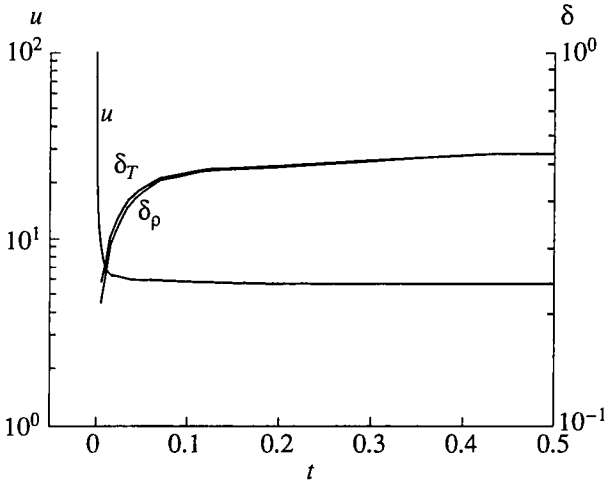

Fig. 2.

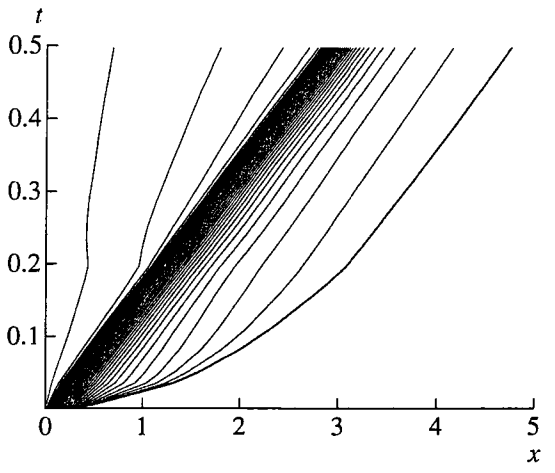

Fig. 3.

$\delta_T(t)$ is equal to the diffusion front width $\delta_\rho(t)$, $\delta_T(t) = \delta_\rho(t)$, and their propagation speed is constant, $u(t) =$ const.

From a computational perspective, steady regimes are characterized by the existence of time-invariant spatial zones of steep gradients of $T(x)$ and $\rho(x)$ propagating from left to right with a constant speed. As the zone of strong variation of the solution develops, the grid nodes are automatically redistributed, condensing in the combustion zone. The values of the gradients determine the minimal spatial mesh size $h_{x,\min}$. The dynamics of variation of h_x can be well characterized by the function $\psi(x_i) = h(x_i)/h(q_i)$ (see Fig. 1c), which is the dimensionless step h_x in the physical space defined as the ratio of a current mesh size to that at the initial moment ($t = 0$, ψ_i). Our computations have shown that the mesh size reduces by approximately ten times in the combustion zone, whereas it increases by a factor of 2–5 in the rest of the domain (see Fig. 1c). In the diagram of node motion, the domain of the most condensed trajectories corresponds to the position of the combustion front (see Fig. 3). Using the results of numerical computations, we obtained the following empirical formula for the combustion rate corresponding to a fixed value of T_a and Le = 1:

$$U = \frac{1.6\sqrt{A}\exp(-0.408\theta)}{\theta},$$

which approximates the results computed for different A and θ within 5%.

Unstable combustion regimes. One of the most important factors of a substantial variation in the combustion temperature is the instability of the flame front. In laminar combustion regimes, the thermodiffusional instability develops when the concentration distribution is not similar to the temperature distribution, i.e., when Le $\neq 1$. The thermodiffusional instability affects the structure of the flame, without inducing any substantial gasdynamic perturbations. The instability becomes stronger as the deviation of the Lewis number from unity increases. As mentioned above, the main destabilizing factor leading to the development of pulsation is the enthalpy excess in the reaction zone. The stabilizing factors include the amount of heat released in the course of combustion and diffusion of mixture components. As either quantity decreases, the pulsation intensity increases. The transition between the regimes corresponds to some critical values of Le and α. The critical conditions for the change of regime have been analyzed in several studies [8–11]. It was shown that, depending on the values of Le and α, the thermodiffusional instability can be either monotone or oscillatory.

When Le $\gg 1$, combustion proceeds in an unstable regime of overheated reacting mixture with enthalpy excess behind the front. As a consequence, the corresponding combustion temperature is higher than the adiabatic one, $T_{\max} > T_a$ (see Fig. 4). The instability is monotone. The highest degree of overheating is attained at initial moments, the subsequent process is characterized by a gradually decreasing propagation velocity (see Fig. 6; in Figs. 4–7, Le = 10, $\theta = 18$, $A = 10^{10}$). Despite the enthalpy excess and the fact that $T_{\max} > T_a$, thermokinetic oscillations are not observed, because they develop only if the characteristic chemical-reaction time is much shorter than the characteristic diffusion time ($t_r \ll t_D$). Since the diffusion layer is wider than the thermal layer ($\delta_\rho(t) > \delta_T(t)$) when Le $\gg 1$ (see Fig. 6), the condition $t_r \ll t_D$ is violated and

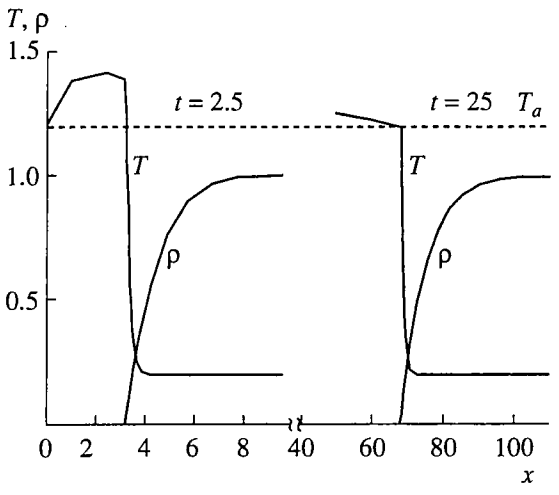

Fig. 4.

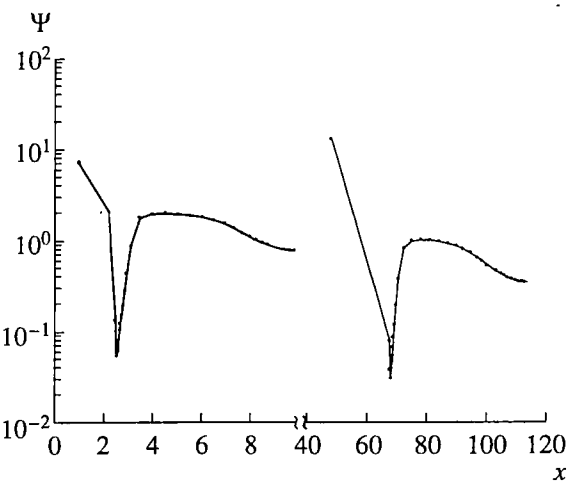

Fig. 5.

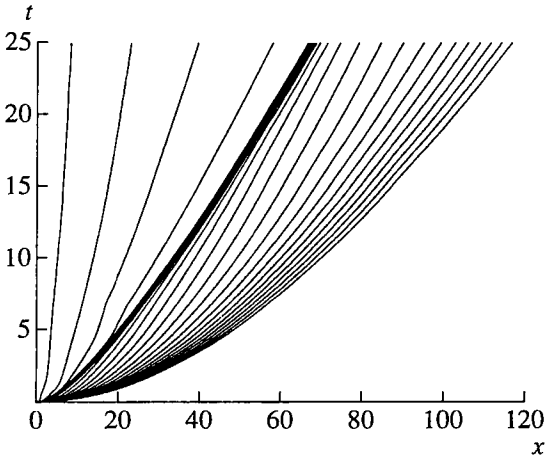

Fig. 6.

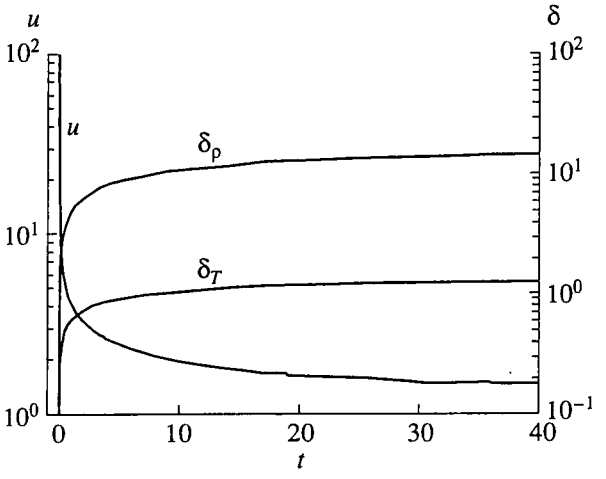

Fig. 7.

thermokinetic oscillations do not develop. From the computational viewpoint, combustion regimes with Le $\gg$ 1 are similar to the regime with Le = 1. As in the case considered above, the adaptive grid condenses in the combustion zone (see Figs. 5, 7). However, the condensed grid is in the steeper front, as the fronts have different widths. When Le $\gg$ 1, the temperature profile $T(x)$ has a greater slope (see Fig. 4).

In gasless combustion (Le = 0), the instability is of a purely thermal nature and is completely determined by the temperature coefficient of the combustion rate α (see [9]): $\alpha = (T_a - T_0)d\ln u/(dT_0) > \alpha_c$. The explicit expression for the temperature coefficient depends on the form of steady combustion law $u(T_a)$. For the Arrhenius dependence of the chemical reaction rate (1), $u \sim \exp[-E/(2RT_a)]$, the stability condition becomes $\alpha = E(T_a - T_0)/(2RT_a^2) < \alpha_c$, $\alpha_c = 4.24$ (see [8, 9]). The value of α_c increases with the Lewis number (0 < Le < 1) [10].

Pulsation dynamics. Numerical simulations have shown that, when the Lewis number is close to unity and Le < 1, the width of the zone of intense chemical reaction is approximately equal to that of the preheat zone, $\delta_\rho(x) \le \delta_T(x)$, and instability of the steady combustion is not observed. However, as the Lewis number decreases, so does the diffusive flux into the combustion zone, and the role of destabilizing factors increases. Marginal combustion instability manifests itself by decaying oscillations (see Fig. 8, where $A = 10^{10}$, $\theta = 18$). As the stability threshold is further exceeded, for example, through an substantial decrease in the Lewis number Le $\ll$ 1, the difference between the characteristic scales $\delta_\rho(x)$ and $\delta_T(x)$ substantially increases, which results in a substantial buildup of excess enthalpy. The excess of heat in the combustion front leads to the onset of a pulsation with increasing amplitude and frequency (see Fig. 8). At certain values

of Le and α, the oscillations become independent of the heating wall and a self-sustained oscillatory combustion regime develops in the system (see Fig. 8). The self-sustained oscillatory combustion front propagates in a sequence of periodically alternating steps of flashes and depressions, which correspond to maximums and minimums of temperature and velocity, respectively (see Fig. 8). In this regime, the velocity of the front propagation is not constant and varies according to a certain law depending on the extent to which the oscillatory-instability threshold is transcended, as determined by the values of Le and α. When the instability is marginal, the combustion rate oscillates almost sinusoidally about its steady value. As the distance from the threshold increases with decreasing Le for a constant α, the pattern of pulsation changes: the oscillation amplitude and frequency increase, the flash duration decreases, and the depression time grows.

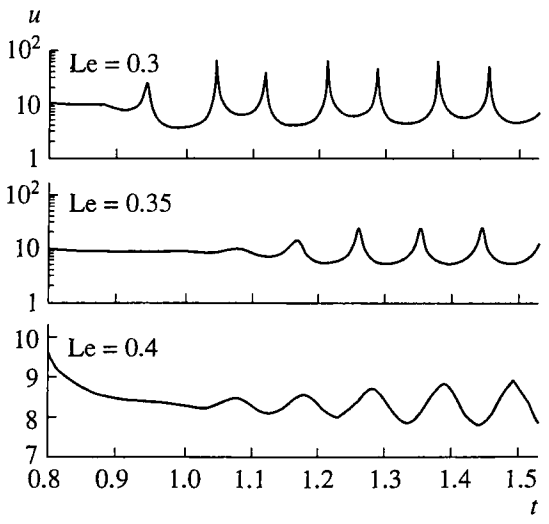

Fig. 8.

Figure 9 shows the spatiotemporal distributions of temperature and density obtained for Le = 0.3, $A = 10^{10}$, and $\theta = 18$. Flashes correspond to moments with odd subscripts; depressions, to those with even subscripts. At the moment of a flash, the temperature beyond the front exceeds that of the steady adiabatic combustion. A temperature peak in Fig. 9a corresponds to a peak of the combustion rate (Fig. 10) and to minima of $\delta_\rho(x)$ and $\delta_T(x)$. High reaction rate results in fast combustion of a preheated layer. As the preheat-zone width decreases, the spatial gradients of T and ρ become steeper (see Figs. 9a, 9b), which stimulates intense heat transfer from the reaction zone and the onset of a depression stage. At the depression stage, the preheated layer is restored by the heat coming from the burned zone; as a consequence, the temperature (and, therefore the combustion rate) beyond the front decreases. By the end of the depression stage, a thick layer of preheated reactant forms, which then burns in a flash again. In the node motion diagram, the oscillation manifests itself by periodic grid condensations (see Fig. 11). The dynamics of the adaptive grid nodes are also characterized by the spatial profiles of ψ plotted for several time moments (see Fig. 12). The function $\psi(x)$ characterizes the variation of the mesh size h_x represented by the ratio of the current distance between adjacent nodes in the physical space to that at $t = 0$. At the flash points, which correspond to peaks of temperature and velocity, the grid nodes are concentrated in the thermal and diffusion fronts At these points, the diagrams of $\psi(x)$ exhibit negative spikes.

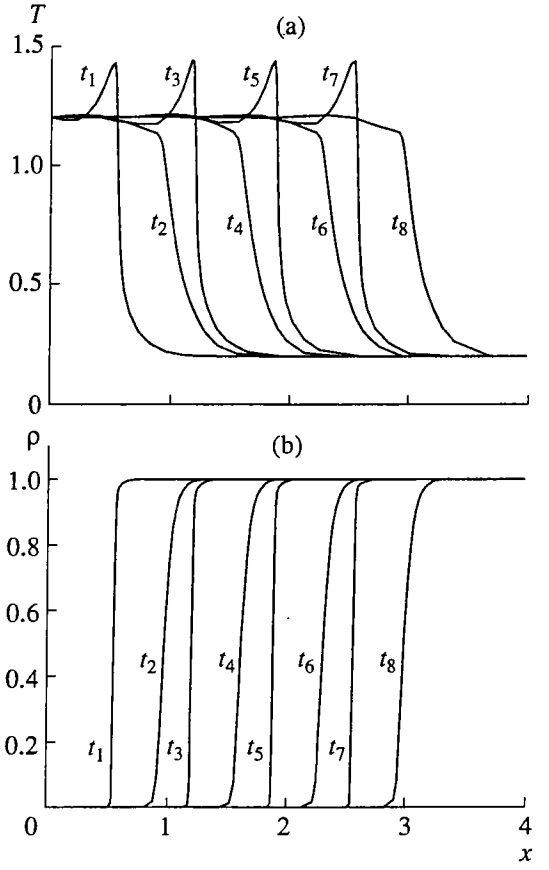

Fig. 9.

Computations showed that self-sustained oscillatory combustion regimes exist in a relatively narrow ranges of Le and α, and the oscillation period can be estimated as $t_a \sim \mathrm{Le}A^{-1}\exp(\theta)$. With further decrease in Le or increase in α, the oscillatory regime breaks down, as its amplitude and frequency increase and the oscillation gradually transforms into relaxation with an increasing duration of the depression stage and shorter flash duration (Fig. 13).

As the Lewis number approaches Le ~ 0.1, pulsation of a complex structure develops, with several velocity peaks observed during each period (see Fig. 13). The complex behavior of the solution predetermines a complicated mechanism of grid adaptation in which the minimal mesh size is reduced by approximately three orders of magnitude (i.e., the value of ψ drops to 10^{-3}). The adaptation complexity is illustrated by the

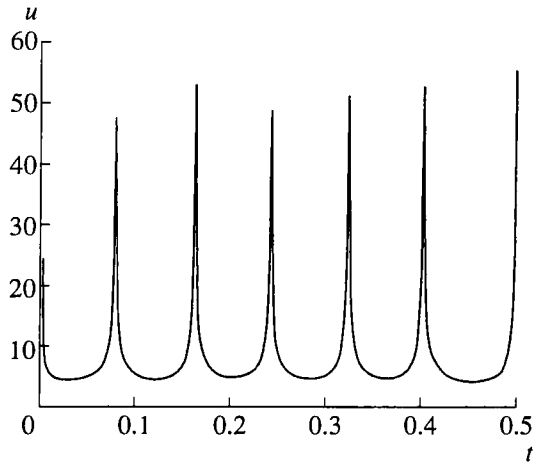

Fig. 10.

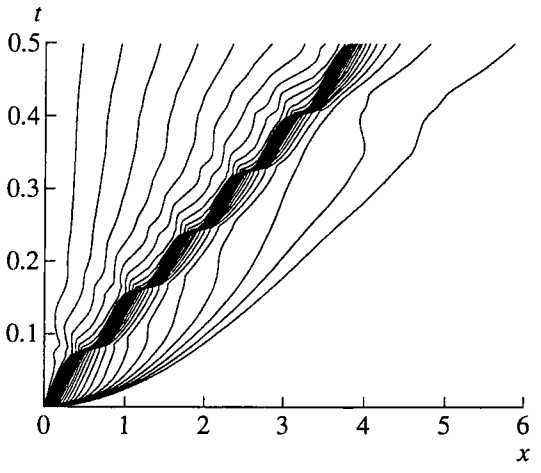

Fig. 11.

diagram of node motion shown in Fig. 14 for Le = 0.1, $A = 10^{10}$, $\theta = 18$, and the total number of nodes $N = 30$.

Finally, we note that pulsating regimes have been observed in a number of experimental studies [22, 23].

6. EFFICIENCY OF THE DYNAMIC ADAPTATION METHOD

The main advantage of adaptive grids is the possibility to perform computations on relatively coarse grids. Let us use the numerical simulations of steady and unsteady regimes of single-stage combustion to obtain quantitative estimates for the efficiency of the dynamic adaptation method. Quantitatively, the efficiency of the method is characterized by the relative run time t_e and the number n_e of nodes employed. The values of $t_e = t_f/t_a$ and $n_e = N_f/N_a$ were determined by comparing the CPU time and number of nodes required in dynamically adaptive algorithms (t_a, N_a) and in those implemented on grids with stationary nodes (t_f, N_f). As a measure of efficiency, we considered the dependence of t_e and n_e on the ratio δ/L of flame width δ to the size L of the computational domain. The flame width and velocity were varied by varying the values of Le and $\alpha(\theta)$. It is obvious that the CPU time and the number of nodes increase with decreasing δ/L.

According to our computations, the minimal number of nodes required to solve a typical combustion problem on an adaptive grid is ~20–30. All subsequent computations on adaptive grids were performed with the same number of nodes, $N = 40$, which proved to be sufficient for conducting a numerical analysis in wide ranges of Le, θ, and A. The computational domain size L was set equal to 10, and the number of nodes in stationary grids was chosen so that the maximal error in velocity did not exceed 1%. For steady combustion regimes, the required accuracy was determined by analyzing the convergence of flame propagation velocity on progressively condensed grids.

To determine the efficiency of grid adaptation under conditions of steady combustion, a series of computations was performed for constant values of $A = 10^8$ and Le = 1 with an activation energy θ varied from 4 to 17.

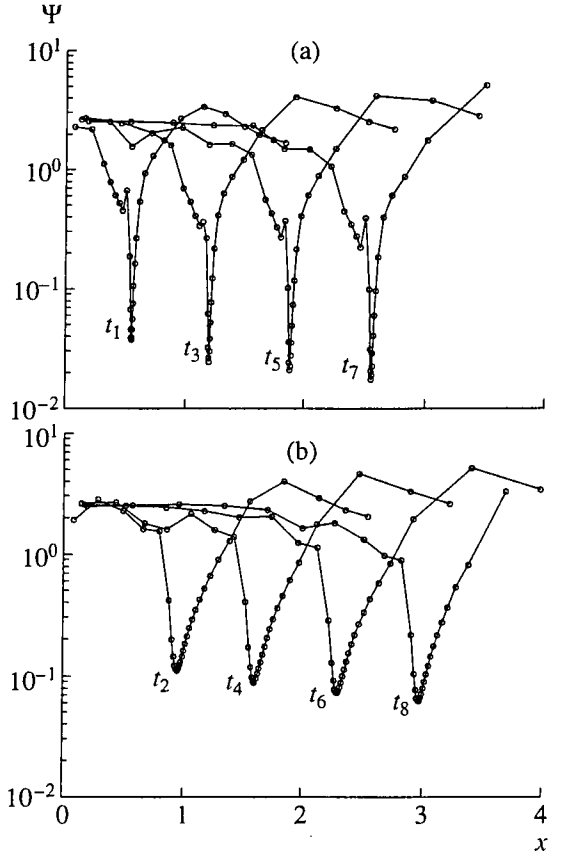

Fig. 12.

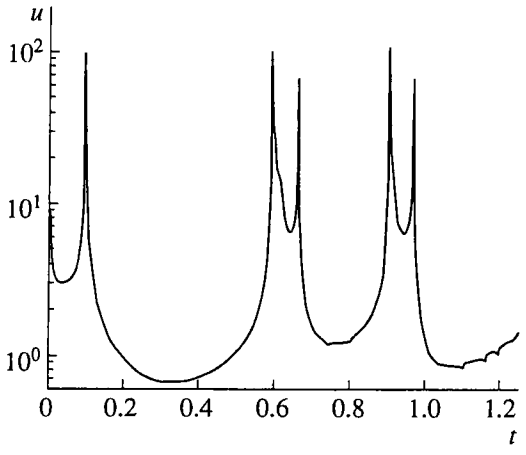

Fig. 13.

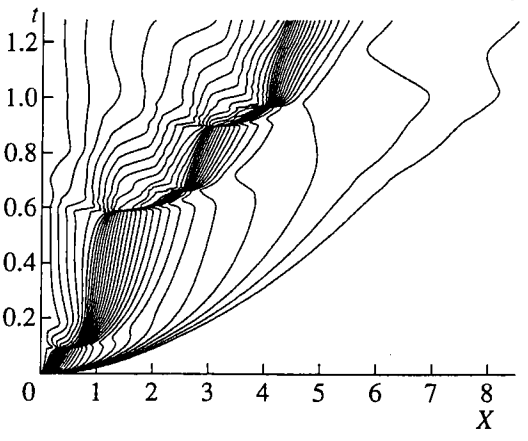

Fig. 14.

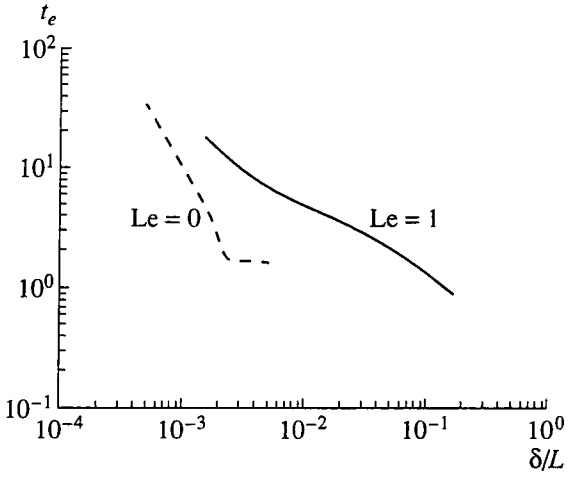

Fig. 15.

The computed results were compared with their counterparts obtained on a grid with fixed nodes. Figure 15 shows the time efficiency t_e as a function of δ/L for regimes with Le = 1. As θ was varied from 17 to 4, the reaction-zone thickness decreased by two orders of magnitude. Accordingly, the ratio of reaction-zone width to domain size $\delta_{\min}/L$ decreased from 0.2 to 2×10^{-3}. The ratio of the required CPU time $t_e = t_f/t_a$ increased from 0.8 to 18. In all computations, the number of nodes in the adaptive grid was held constant ($N_a = 40$), whereas the number of fixed increased from $N_f = 500$ to 6000. Thus, in computing steady combustion regimes, the efficiency $n_e = N_f/N_a$ of dynamic adaptation with respect to the required number of nodes is varied from 10 to 150. The time efficiency of dynamic adaptation algorithms can be as high as $t_e \approx 20$. However, when the size of a combustion zone is comparable to the domain size, the time efficiency of adaptive meshing noticeably decreases. Moreover, when $\delta/L \approx 0.2$, algorithms implemented on grids with fixed nodes become more advantageous (by ≈20%).

The efficiency of dynamic adaptation in unsteady combustion regimes was analyzed for Le = 0. In Fig. 15, the dashed curve represents the dependence $t_e(\delta_{\min}/L)$, which characterizes the time efficiency of dynamic adaptation for Le = 0. The neighborhood of $\delta/L \approx 2 \times 10^{-3}$ in the graph of $t_e(\delta_{\min}/L)$ corresponds to the transition between a steady combustion regime ($\theta \le 10$) and an oscillatory regime ($\theta > 10$). The time efficiency of dynamic adaptation in the oscillatory regime ($\delta/L > 2 \times 10^{-3}$, $\theta > 0$) noticeably decreases because of the relatively frequent and substantial grid adjustments at the moments of flashes and depressions. At these moments, the reaction-zone width changes by a factor of several tens or hundreds. Transition to a steady regime ($\delta/L < 2 \times 10^{-3}$, $\theta \le 10$) is associated with an increase in the efficiency index $t_e(\delta_{\min}/L)$,

which rapidly attains a value ≈30. The efficiency of grid adaptation with respect to the required number of nodes is particularly well manifested in oscillatory regimes. In the examples discussed here, the parameter $n_e = N_f/N_a$ reached values ≈500.

Note that these estimates were obtained for a computational domain of fixed size $L = 10$. As the domain size is increased, the advantage of adaptive meshing in terms of time efficiency increases further, approximately as L^q, where $q = 0.4$–0.5.

CONCLUSION

Experiments show [6, 22] that most industrial combustion systems make use of layer-by-layer regimes, which are additionally complicated by turbulence and fuel–oxidizer mixing. However, both the laminar and layer-by-layer combustion waves are driven by the thermodiffusional mechanism of propagation of chemical reactions. The analysis presented in this paper is focused on typical steady and pulsating combustion regimes and their characteristic features. The results obtained show that the dynamic adaptation method can be successfully applied in numerical simulations of laminar combustion problems in wide ranges of Le and θ characteristic of both steady and pulsating regimes. The method is quite efficient. Its application allows one to reduce the number of nodes by 1–2.5 orders of magnitude and raise the time efficiency by 2–50 times, which can be especially important for multidimensional simulations.

ACKNOWLEDGMENTS

This work was supported by the Russian Foundation for Basic Research, project no. 01-00604 and by the Russian Foundation for Basic Research–Belorussian Foundation for Basic Research, project no. 00-01-81065 Bel 2000a.

REFERENCES

1. *Modeling, Mesh Generation, and Adaptive Numerical Methods for Partial Differential Equations*, Babuska, I., Henshaw, W.D., Oliger, J.E., *et al.*, Eds., New York: Springer, 1995.
2. Thomphson, J.F., Warsi, Z.U.A., and Mastin, C.W., *Numerical Grid Generation: Foundations and Applications*, New York: North-Holland, 1985.
3. Mazhukin, V.I. and Takoeva, L.Yu., Principles of Dynamically Adaptive Gird Generation in One-Dimensional Boundary Value Problems, *Mat. Modelirovanie*, 1990, vol. 2, no. 3, pp. 101–118.
4. Liseikin, V.D., Review of Adaptive Structured Grid Generation, *Zh. Vychisl. Mat. Mat. Fiz.*, 1996, vol. 36, no. 1, pp. 3–41.
5. Ivanenko, S.A. and Prokopov, G.P., Adaptive Harmonic Grid Generation Methods, *Zh. Vychisl. Mat. Mat. Fiz.*, 1999, vol. 37, no. 6, pp. 643–662.
6. Lewis, B. and von Elbe, G., *Combustion, Flames, and Explosions of Gases*, New York: Academic, 1961. Translated under the title *Gorenie, plamya i vzryvy v gazakh*, Moscow: Mir, 1968.
7. Zel'dovich, Ya.B., Barenblatt, G.I., Librovich, V.B., and Makhviladze, G.M., *Matematicheskaya teoriya goreniya i vzryva* (Mathematical Theory of Combustion and Explosions), Moscow: Nauka, 1980.
8. Shkadinskii, K.G., Khaikin, B.I., and Merzhanov, A.G., Propagation of a Pulsating Exothermal Reaction Front in a Condensed Phase, *Fiz. Goreniya Vzryva*, 1971, vol. 7, no. 1, pp. 19–28.
9. Makhviladze, G.M. and Novozhilov, B.V., Two-Dimensional Stability of Combustion in Condensed Systems, *Zh. Prikl. Mekh. Tekhn. Fiz.*, 1971, no. 5, pp. 51–59.
10. Grishin, A.M., Bertsun, V.N., and Agranat, V.M., Analysis of the Thermodiffusional Instability of Laminar Flames, *Dokl. Akad. Nauk SSSR*, 1977, vol. 235, no. 3, pp. 550–553.
11. Grishin, A.M. and Zelenskii, E.E., Analysis of the Thermodiffusional Instability of Laminar Flames, *Chisl. Metody Mekh. Sploshnoi Sredy*, Novosibirsk, 1977, vol. 8, no. 4, pp. 5–19.
12. Dar'in, N.A. and Mazhukin, V.I., Mathematical Modeling of the Stefan Problem on an Adaptive Grid, *Diff. Uravn.*, 1987, vol. 23, no. 7, pp. 1154–1160.
13. Dar'in, N.A. and Mazhukin, V.I., On One Approach to Adaptive Grid Generation, *Dokl. Akad. Nauk SSSR*, 1988, vol. 298, no. 1, pp. 64–68.
14. Dar'in, N.A., Mazhukin, V.I., and Samarskii, A.A., Finite-Difference Method for Solving Gas-Dynamics Equations Using Adaptive Grids Dynamically Tied to the Solution, *Zh. Vychisl. Mat. Mat. Fiz.*, 1988, vol. 28, no. 8, pp. 1210–1225.
15. Breslavskii, P.V. and Mazhukin, V.I., Mathematical Modeling of Pulsed Melting and Evaporation with Explicit Representation of Phase Boundaries, *Inzh.-Fiz. Zh.*, 1989, vol. 57, no. 1, pp. 107–114.

16. Mazhukin, V.I., Smurov, I., Dupuy, C., and Jeandel, D., Simulation of Laser Induced Melting and Evaporation Processes in Superconducting Ceramics, *Numer. Heat Transfer: Appl.,* 1994, vol. 26, pp. 587–600.
17. Mazhukin, V.I., Samarskii, A.A., and Shapranov, A.A., Dynamic Adaptation Method in the Burgers Problem, *Dokl. Akad. Nauk*, 1993, vol. 333, no. 2, pp. 165–169.
18. Breslavskii, P.V. and Mazhukin, V.I., Dynamic Adaptation Method for Problems in Gas Dynamics, *Mat. Modelirovanie*, 1995, vol. 7, no. 12, pp. 48–78.
19. Otey, G.R. and Dwyer, H.A., Numerical Study of the Interaction of Fast Chemistry and Diffusion, *AIAA J.*, 1979, vol. 17, no. 6, pp. 606–613.
20. Vasilevskii, V.F. and Mazhukin, V.N., Numerical Analysis of Temperature Waves with Weak Discontinuities on Dynamically Adaptive Grids, *Diff. Uravn.*, 1989, vol. 25, no. 7, pp. 1188–1193.
21. Samarskii, A.A., *Teoriya raznostnykh skhem* (Theory of Finite-Difference Schemes), Moscow: Nauka, 1989.
22. Shchetinkov, E.S., *Fizika goreniya gazov* (Physics of Gaseous Combustion), Moscow: Nauka, 1965.
23. Merzhanov, A.G., Filonenko, A.K., and Borovinskaya, I.P., New Phenomena in Combustion of Consdensed Systems, *Dokl. Akad. Nauk SSSR*, 1973, vol. 208, no. 4, pp. 892–894.